Geophysical Research Letters

RESEARCH LETTER
10.1029/2023GL103426

Effects of Lake Baikal on Summertime Precipitation Climatology Over the Lake Surface

Hyunho Lee[1], Gantuya Ganbat[2], Han-Gyul Jin[3], Jaemyeong Mango Seo[4], Sungju Moon[5], Hyejeong Bok[6], and Jong-Jin Baik[3]

[1]Department of Atmospheric Science, Kongju National University, Gongju, South Korea, [2]Faculty of Raw Materials and Environmental Engineering, German-Mongolian Institute for Resources and Technology, Ulaanbaatar, Mongolia, [3]School of Earth and Environmental Sciences, Seoul National University, Seoul, South Korea, [4]Max-Planck Institute for Meteorology, Hamburg, Germany, [5]Department of Data, Media, and Design, Nevada State College, Henderson, NV, USA, [6]Numerical Modeling Center, Korea Meteorological Administration, Daejeon, South Korea

Key Points:

- We conducted two 15-year cloud-resolving simulations to investigate how Lake Baikal affects summertime surface precipitation over it
- A decrease in air temperature weakens convection over the lake, reducing precipitation by 15% as well as water vapor amount
- It is essential to consider complex interactions among clouds, radiation, and lake surfaces to characterize the lake effect

Supporting Information:

Supporting Information may be found in the online version of this article.

Correspondence to:

G. Ganbat and J.-J. Baik,
gantuya@gmit.edu.mn;
jjbaik@snu.ac.kr

Citation:

Lee, H., Ganbat, G., Jin, H.-G., Seo, J. M., Moon, S., Bok, H., & Baik, J.-J. (2023). Effects of Lake Baikal on summertime precipitation climatology over the lake surface. *Geophysical Research Letters*, *50*, e2023GL103426. https://doi.org/10.1029/2023GL103426

Received 23 FEB 2023
Accepted 2 MAY 2023

Abstract This study investigates the impacts of Lake Baikal, the largest by volume and the deepest freshwater lake in the world, on its nearby precipitation climate. Satellite observations and a reanalysis data set reveal that summertime precipitation amount is smaller over Lake Baikal than around it. A 15-year regional climate simulation at a cloud-resolving scale supports the smaller precipitation, and another simulation in which the lake is replaced by forest shows that the lake reduces summertime precipitation over it by 15%. The lake decreases daytime near-surface air temperature, resulting in more convectively stable atmosphere over the lake. Latent heat flux is reduced along with the weakened convection, and the lower-level moisture convergence and upper-level moisture divergence over the lake are weakened.

Plain Language Summary Lakes can have profound impacts on local precipitation, and such impacts are influenced by a variety of factors including the lake's geographical location, its size, and its depth. If only because of its sheer size, the question of how Lake Baikal, the largest and deepest freshwater lake in the world, affects the local climate deserves an in-depth investigation. The present study aims to tackle this question by simulating the regional climate with and without Lake Baikal present, focusing on the summertime precipitation. The simulation results indicate that Lake Baikal reduces the summertime precipitation by 15%. It turns out that the lake cools down the atmosphere near the surface, which weakens convection. Moisture supply from the surface to the atmosphere is rather reduced due to the lake. This study suggests that the role of a lake, especially that as large as Lake Baikal, in regional climate can be more complicated than previously understood due to the complex interactions among multiple different processes involving convective instability, moisture supply, and atmospheric radiation.

1. Introduction

Lakes reduce temporal variations in near-surface air temperature because the heat capacity of water is larger than that of the surrounding land and can increase the amount of water vapor in the atmosphere above them through active evaporation from their surface. Owing to the thermal and humidity contrasts between a lake and its surrounding area, a lake can be anticipated to modulate weather and impact climate around it (Camberlin et al., 2018; Laird et al., 2009).

Lake-induced changes in precipitation vary depending on factors such as season and geographical location of a lake. Since the atmosphere over the lake is generally warmer and more humid than that over the surrounding land in winter unless the lake is ice-covered, convection over the lake becomes more active and snowfalls prevail on the downwind side of the lake. This is referred to as lake-effect snow, readily observed for many lakes (e.g., Peace & Sykes, 1966; Steenburgh et al., 2000). In summer, on the other hand, the cool lake surface stabilizes the lower atmosphere over it, which reduces convective clouds and precipitation over the lake and its downwind area (e.g., Gu et al., 2016; Lyons, 1966). Such seasonally reversed lake effects on precipitation have been reported for midlatitude lakes such as the Great Lakes in North America (Notaro et al., 2013) and Lake Ladoga in Europe (Samuelsson et al., 2010). However, the African Great Lakes in the tropics, where neither warm nor cold seasons exist, exhibit substantial lake-induced increases in over-lake precipitation during wet seasons. This is attributed to the lake surface having ~2.5 times greater moisture flux than the moisture flux from the equivalent land surface (Thiery et al., 2015). For lakes located in basins such as Lake Victoria, the terrain surrounding the lakes plays

key roles in precipitation over and around the lakes by inducing mesoscale circulation and modifying the synoptic flow (Van de Walle et al., 2020). To reveal the effects of a lake on precipitation, various physical processes such as differential heating, evaporation, convection, radiation, and mesoscale circulation and their complicated interactions should be considered.

Lake Baikal located in southeastern Siberia, Russia has received relatively little attention compared to other lakes despite its geographic uniqueness. Lake Baikal is a freshwater lake with its center at 53.3°N and 108.0°E. Formed over 25–30 million years ago, Lake Baikal is the largest by volume and the deepest lake in the world with its maximum depth of 1,642 m. At 23,600 km^3, its volume is larger than the volumes of all five of the Great Lakes in North America combined (Dabaeva et al., 2016). Because of its geographical location and its depth, it is usually covered with ice until late spring and its surface temperature is generally lower than 20°C even in summer, producing a large contrast in surface temperature between the lake and the nearby land (Kouraev et al., 2007, 2021). In the region where Lake Baikal is located, the contribution of large-scale precipitation associated with extratropical synoptic storms to the total precipitation in summertime is slightly greater than 50% (Hawcroft et al., 2012), which suggests that both large-scale precipitation and local-scale convective precipitation are important in this region. This study explores lake-induced changes in summertime precipitation over Lake Baikal. To the authors' best knowledge, this is the first study to assess the impacts of Lake Baikal on summertime precipitation.

2. Methods

To find the climatic characteristics of precipitation distributions for Lake Baikal and the surrounding area where high-resolution rain gauge data are not available, we analyze five satellite-based precipitation estimation data sets: Precipitation Estimation from Remotely Sensed Information using Artificial Neural Networks-Climate Data Record (PERSIANN-CDR; Ashouri et al., 2015), Integrated Multi-satellitE Retrievals for GPM-Final (IMERG-Final; Huffman et al., 2020), Climate prediction center MORPHing technique-Climate Data Record (CMORPH-CDR; Xie et al., 2017), Global Satellite Mapping of Precipitation (GSMaP; Kubota et al., 2020), and Multi-Source Weighted-Ensemble Precipitation (MSWEP; Beck et al., 2019). The data sets provide global high-resolution precipitation estimations covering the 60°S–60°N latitude band. In addition, the European Centre for Medium-Range Weather Forecasts Reanalysis version 5 (ERA5, Hersbach et al., 2020) data set is also analyzed.

To investigate the role of Lake Baikal in summer precipitation around it, we conduct two 15-year simulations using a cloud-resolving model, the Weather Research and Forecasting (WRF) model version 4.2.1 (Skamarock et al., 2019) that solves a fully compressible nonhydrostatic governing equation system. The WRF model employs the lake model obtained from the Community Land Model version 4.5 with some modifications by Gu et al. (2015) in which a 1-D lake water column is divided into 10 layers. We modify the vertical grid spacings to increase exponentially with depth. The lake model evaluates the surface parameters for lakes, and the Noah land surface model (Tewari et al., 2004) does so for non-lake surfaces. We use two one-way nested domains configured via the Lambert conformal map projection with the horizontal grid spacings of 15 and 5 km, respectively, and the horizontal domain sizes of 3,000 km × 3,000 km and 1,545 km × 1,050 km, respectively (Figure S1a in Supporting Information S1). Each domain has the top at 10 hPa and is vertically divided into 45 layers. National Centers for Environmental Prediction (NCEP) final analysis data (Kalnay et al., 1996) provide the initial and boundary conditions for the outer domain. The initial lake water temperature linearly changes with depth until 50 m below the lake surface where the water temperature is 4°C. The model is integrated from 25 May 00 UTC in each year from 2005 to 2019, and the analysis is performed for June, July, and August. A spectral nudging provided by the WRF model is used for the seasonal hindcast. The parameterizations of physical processes used in this study are listed in Table S1 in Supporting Information S1.

For each year, two simulations are conducted. The LAKE simulation considers Lake Baikal as is, whereas the NOLAKE simulation replaces the land type of the lake area by mixed forest, which is the most common land type around Lake Baikal (Figure S1b in Supporting Information S1). Moderate Resolution Imaging Spectroradiometer (MODIS) 30″ data set (Hansen et al., 2000) is used to set the land type of each grid cell. In the WRF model used in this study, water body has an albedo of 0.08 and an emissivity of 0.98, and mixed forest has an albedo of 0.13 and an emissivity of 0.97.

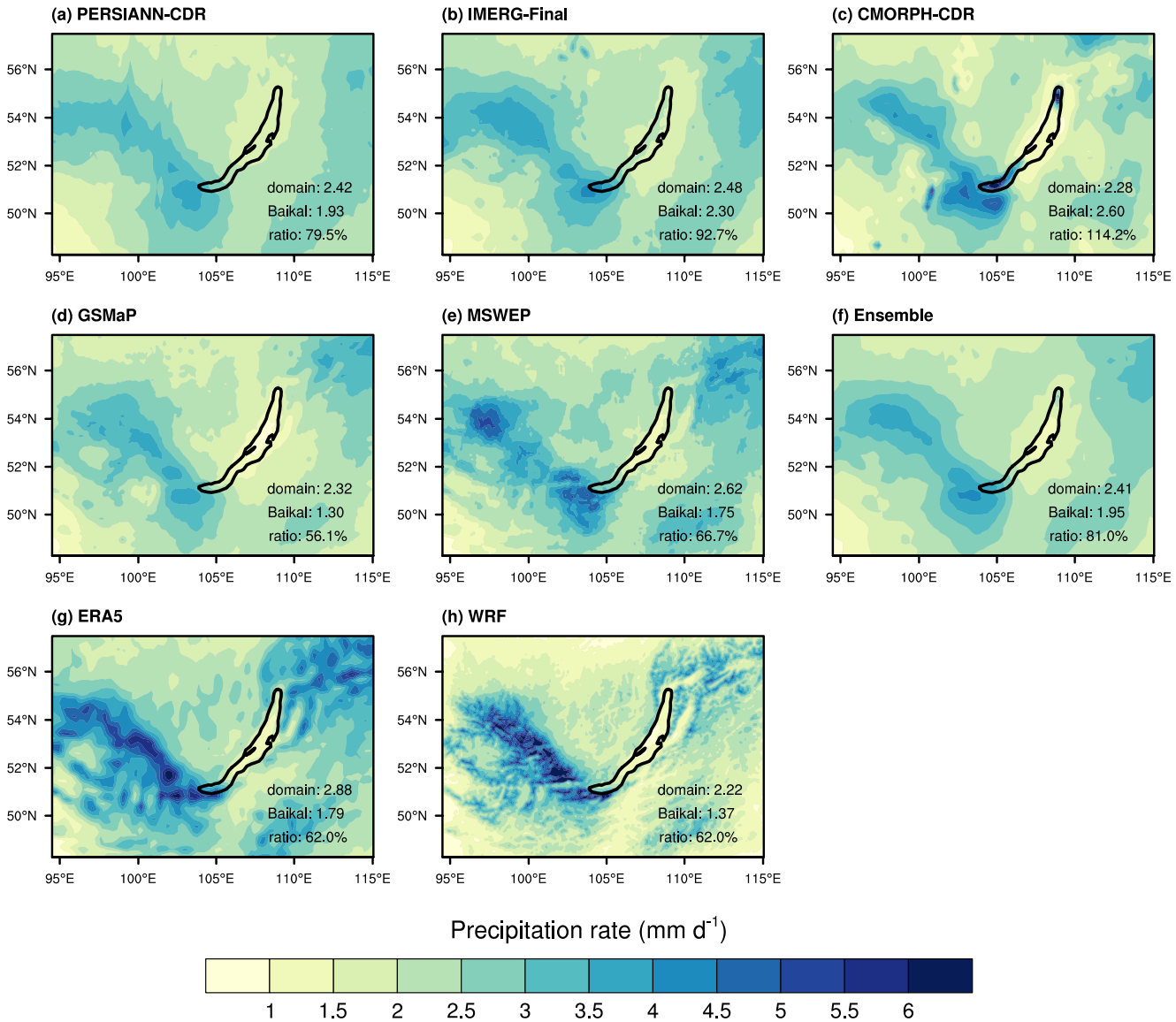

Figure 1. Fields of surface precipitation rate averaged over June, July, and August during 2005–2019 obtained from (a) PERSIANN-CDR, (b) IMERG-Final, (c) CMORPH-CDR, (d) GSMaP, (e) MSWEP, (f) the average of satellite-based data sets [(a)–(e)], (g) ERA5, and (h) the reference model simulation (the LAKE simulation). The precipitation rates over Lake Baikal and the domain (units: mm d^{-1}) and their ratio are given in each panel.

3. Results and Discussion

Figure 1 shows the summertime (June, July, and August) precipitation in the region around Lake Baikal averaged over 15 years from 2005 to 2019 obtained using the precipitation estimations and the LAKE simulation. The majority of the satellite-based estimations (PERSIANN-CDR, GSMaP, and MSWEP) and the ERA5 reanalysis reveal that the summertime precipitation amount over Lake Baikal is smaller than that in the surrounding land area and that this reduction is more pronounced in the northern part of the lake. We note that Nicholson et al. (2021) argued that IMERG-Final tends to overestimate the precipitation over inland water bodies and attributed the likely causes to the passive microwave assessments of strong convection. The ensemble average of the satellite-based estimations exhibits that the averaged summertime surface precipitation rate over Lake Baikal is 1.95 mm d^{-1}, which is 81% of that in the domain.

The LAKE simulation, which serves as the reference, adequately reproduces the estimated summertime precipitation climatology over Lake Baikal (Figure 1h). In the simulation, the precipitation rate is smaller over the lake than in the surrounding area, and this smaller precipitation is more pronounced in the northern part of the

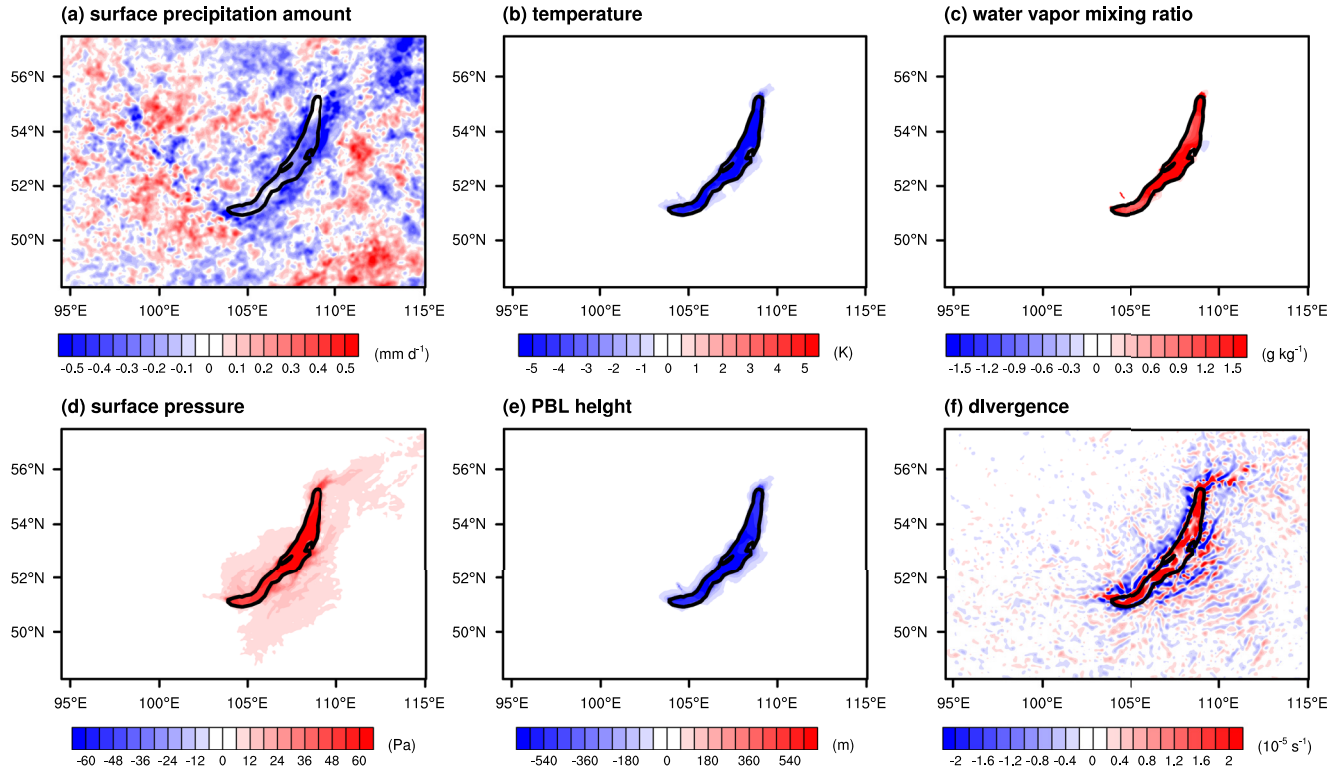

Figure 2. Fields of differences in (a) surface precipitation rate, (b) 2-m air temperature, (c) 2-m water vapor mixing ratio, (d) surface pressure, (e) planetary boundary layer (PBL) height, and (f) horizontal divergence of wind velocity between the LAKE and NOLAKE simulations (LAKE—NOLAKE). (f) is evaluated at the first model level.

lake, which is consistent with the satellite-based estimations. Averaged over the lake, the precipitation rate in the simulation is 1.37 mm d^{-1}, which is 62% of that in the domain. The ratio of surface precipitation over the lake to the domain-averaged precipitation in the simulation is similar to those of GSMaP (56%), MSWEP (67%), and ERA5 (62%). We note that the NOLAKE simulation also exhibits a smaller precipitation rate over the original lake area than in the surrounding area (not shown), which suggests that factors other than the presence of the lake such as the basin topography where the inversion layer can form frequently also play a role in the reduction of precipitation over the lake.

A further analysis using the ERA5 reanalysis shows that convective precipitation and large-scale precipitation are within the similar order of magnitude in the domain (Figure S2 in Supporting Information S1), which roughly reproduces the result of Hawcroft et al. (2012). If we focus on the area of Lake Baikal only, convective precipitation is smaller than large-scale precipitation there. An additional simulation that is identical to the LAKE simulation except applying the cumulus parameterization in the outer domain to the inner domain also reveals that convective precipitation is smaller than large-scale precipitation over the lake surface.

In addition to the surface precipitation rates, time series of lake surface water temperature (LSWT) and vertical profiles of pressure, temperature, water vapor mixing ratio, and equivalent potential temperature (EPT) are also compared to observations (Figures S3 and S4 in Supporting Information S1). The model tends to overestimate the LSWT by a few degrees. Except for this difference, the simulation adequately captures the observed characteristics such as the highly stable near-surface atmospheric layer (Figures S4b and S4d in Supporting Information S1).

It is difficult to assess whether this reduction in precipitation amount over the lake is solely attributable to the lake because the reduction can also be caused by the region's topographic characteristics such as having relatively low altitudes compared to the surrounding mountains (Figure S1 in Supporting Information S1). The extent to which Lake Baikal is responsible for the smaller precipitation amount over the lake can be deduced from comparisons between precipitation in the LAKE and NOLAKE simulations. The precipitation rate averaged over the lake area in the LAKE simulation is 15% smaller than that in the NOLAKE simulation (Figure 2a). Despite its interannual

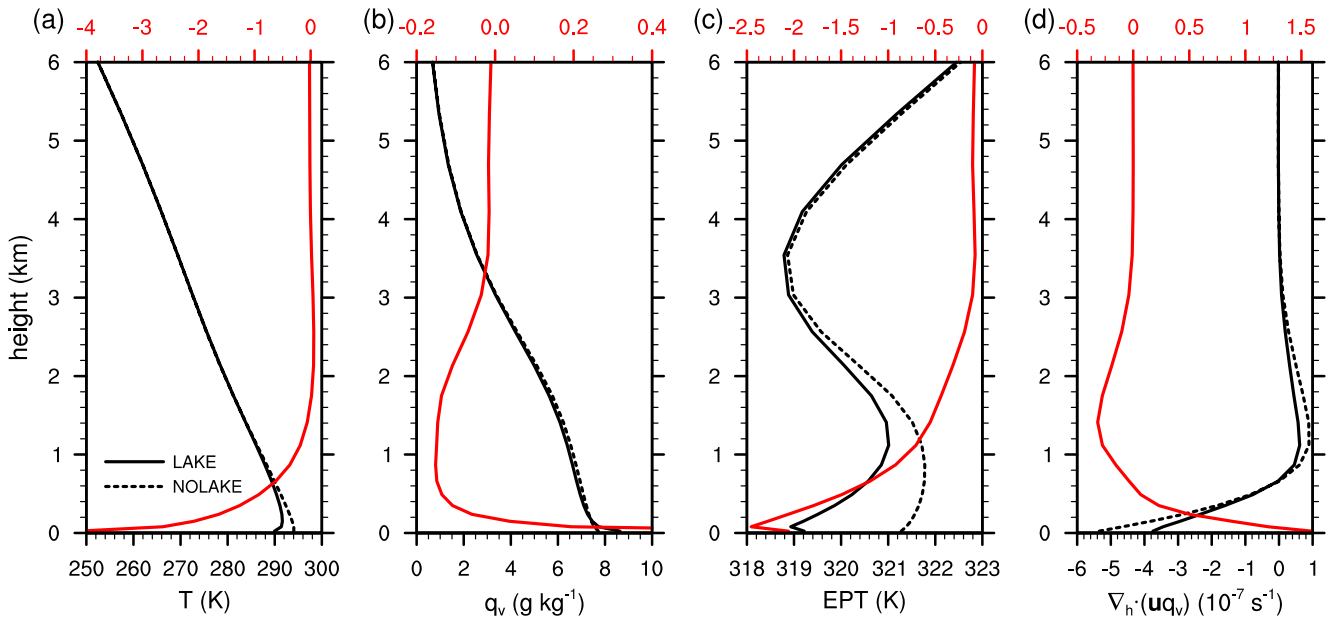

Figure 3. Vertical profiles of (a) temperature, (b) water vapor mixing ratio, (c) EPT, and (d) horizontal divergence of water vapor transport averaged over the Lake Baikal area in the LAKE (solid line) and NOLAKE (dashed line) simulations. The red solid line in each panel indicates the difference between the LAKE and NOLAKE simulations (LAKE—NOLAKE). The vertical coordinate is above ground level (AGL); the height at the lake surface is zero.

variability, the decrease in summertime precipitation amount is seen in all simulations for every year except 2014 (Figure S5 in Supporting Information S1). The changes in precipitation induced by the lake are not confined to the lake area but are spread throughout the domain. In some areas, such as the area far east of the lake (~49°N, 112°E), precipitation is greater in the LAKE simulation than in the NOLAKE simulation. As to why the lake induces the increases in precipitation amounts in these areas, further in-depth research is required.

To understand how Lake Baikal alters the thermodynamic and dynamic states of the atmosphere and accordingly suppresses summertime precipitation, some relevant atmospheric quantities such as temperature, water vapor mixing ratio, surface pressure, planetary boundary layer (PBL) height, and divergence are analyzed (Figures 2b–2f). Differences in some atmospheric quantities (e.g., temperature, water vapor mixing ratio, and PBL height) are substantially confined to the lake area, whereas the other quantities (e.g., surface pressure and divergence) additionally show relatively small but non-negligible changes outside the lake area. The near-surface air temperature averaged over the lake area is reduced by 5.0°C. The lake lowers the near-surface air temperature largely owing to the larger heat capacity of water than that of land. This decrease in near-surface air temperature induces higher surface pressure and thus weaker low-level convergence, which weakens convection over the lake. The decreased near-surface air temperature also causes a more stable atmosphere thus decreased vertical turbulent mixing, which is revealed through a decrease in PBL height. As expected, the lake humidifies the near-surface atmosphere over it. The near-surface water vapor mixing ratio averaged over the lake area is higher in the LAKE simulation than in the NOLAKE simulation by 1.5 g kg^{-1}.

To examine the vertical extent of the lake-induced changes and the propagation of the lake-induced changes toward upper layers, the vertical structures of atmospheric quantities are analyzed (Figure 3). The temperature is lower in the LAKE simulation, and the cooling effect of the lake extends up to $z \sim 2$ km. The water vapor mixing ratio near the surface is higher in the LAKE simulation than in the NOLAKE simulation, as already examined. However, the higher water vapor mixing ratio is limited to the atmospheric layer very close to the surface; the water vapor mixing ratio is lower in the LAKE simulation above $z \sim 200$ m, and the difference is visible up to $z \sim 3$ km. This drier environment in the LAKE simulation implies that the suppression of convection reduces the upward transport of water vapor and that the evaporation from the lake surface does not effectively supply water vapor to the atmosphere above.

The EPT is lower in the LAKE simulation than in the NOLAKE simulation in the layer below $z < \sim 3$ km (Figure 3c). In the LAKE simulation, the EPT increases with height up to $z \sim 1.1$ km except the first model

layer with an average rate of 2.0 K km^{-1}, showing the existence of a convectively stable layer. In the NOLAKE simulation, the EPT also increases with height in the lower atmosphere as in the LAKE simulation but up to a lower level ($z \sim 0.9$ km) and at a smaller rate (0.6 K km^{-1}) compared to the LAKE simulation. This suggests that the convectively stable layer in the lower atmosphere is thicker and more stable in the LAKE simulation than in the NOLAKE simulation. Above the convectively stable layer, a convectively unstable layer, which is a favorable condition for the development of convection, extends up to $z \sim 3.5$ km in both simulations. However, the convectively unstable layer is shallower and less unstable in the LAKE simulation than in the NOLAKE simulation. The analysis results obtained from the vertical profiles of EPT suggest that convection over the lake is suppressed and that relatively deeper convection would be developed if there were no lake.

Figure 3d shows the vertical profiles of horizontal divergence of water vapor transport, $\nabla_h \cdot (\boldsymbol{u} q_v)$, where ∇_h is the horizontal del operator, $\boldsymbol{u}$ is the horizontal wind velocity, and q_v is the water vapor mixing ratio. In both simulations, water vapor converges in the lower layer ($z < 0.7$ km) and diverges in the upper layer (0.7 km $< z <$ 3.5 km), which represents a typical feature over a basin topography (e.g., Satyamurty et al., 2013). Since this is also seen in the NOLAKE simulation, this feature is thought to be caused by the common geographical features shared by both simulations. Compared to the NOLAKE simulation, both the lower-level convergence and the upper-level divergence are weaker in the LAKE simulation, also indicating weakened convection over the lake (see also Figure 2f). The convergence of water vapor transport in the lower layer is 19% less in the LAKE simulation than in the NOLAKE simulation. This weaker convergence reduces convective available energy in the lower atmosphere, which can further weaken convection. Note that the decrease in divergence of water vapor transport in the upper layer is greater than the decrease in convergence of water vapor transport in the lower layer, indicating an increase in the convergence of net lateral fluxes of water vapor mixing ratio in the column over the lake.

The net radiative flux at the surface is greater in the LAKE simulation than in the NOLAKE simulation, mainly attributable to the less outgoing shortwave radiation due to the lower albedo of water and the less outgoing longwave radiation due to the lower surface temperature (Figure 4a and more detail in Figure S6 in Supporting Information S1). In addition, in the LAKE simulation, the sensible heat flux is from the atmosphere to the surface throughout the day (Figure 4b). The atmosphere near the surface is, therefore, stable so that convection over the lake is more likely to be inhibited. In the NOLAKE simulation, on the other hand, the direction of sensible heat flux is upward in the daytime and downward in the nighttime. Contrary to the expectation that a lake would enhance evaporation and thus increase the latent heat flux, the daytime latent heat flux is smaller in the LAKE simulation than in the NOLAKE simulation (Figure 4c), despite the lower soil moisture in the mixed forest surface than in the lake. In the NOLAKE simulation, the sensible and latent heat fluxes are the two major terms that distribute the net incoming radiative flux. However, in the LAKE simulation, most of the net incoming radiative flux is distributed by the heat flux descending into the deep lake water. We note that the water temperature below ~100 m depth from the lake surface remains constant at 4°C because of the sheer depth of Lake Baikal.

The more stable near-surface atmosphere in the LAKE simulation (Figure 3c) reduces the upward escape of near-surface water vapor, contributing to the smaller latent heat flux in the LAKE simulation. The lake-induced reduction in latent heat flux contributes to the decrease in over-lake precipitable water and hence to the decreases in condensed water and precipitation (Figures 4d–4f). Similar result has been reported for several midlatitude lakes during the summer months such as the Great Lakes (Notaro et al., 2013), Lake Taihu (Gu et al., 2016), and Lake Ladoga (Samuelsson et al., 2010). On the contrary, for the African Great Lakes located in the tropics, the presence of lakes substantially increases the latent heat flux and over-lake precipitation regardless of season (Thiery et al., 2015).

Diurnal variation of surface precipitation rate in both simulations shows a common pattern of decreasing in the morning, reaching the minimum around noon, and increasing afterward for some hours (Figure 4f). In the NOLAKE simulation, the surface precipitation rate increases significantly in the afternoon and remains high between 15 LT and midnight. However, unlike in the NOLAKE simulation, in the LAKE simulation, the diurnal maximum in precipitation rate no longer occurs in the afternoon. Such trend is also readily seen in the diurnal variations of the precipitable water and the condensed water (Figures 4d and 4e). That the lake-induced reduction in surface precipitation rate is concentrated in the afternoon and evening implies that the lake mainly reduces convective precipitation.

The vertical profiles of mixing ratios of all hydrometeor types reveal that deep mixed-phase clouds having a higher snow mixing ratio than the graupel mixing ratio are prevalent in both the LAKE and NOLAKE simulations

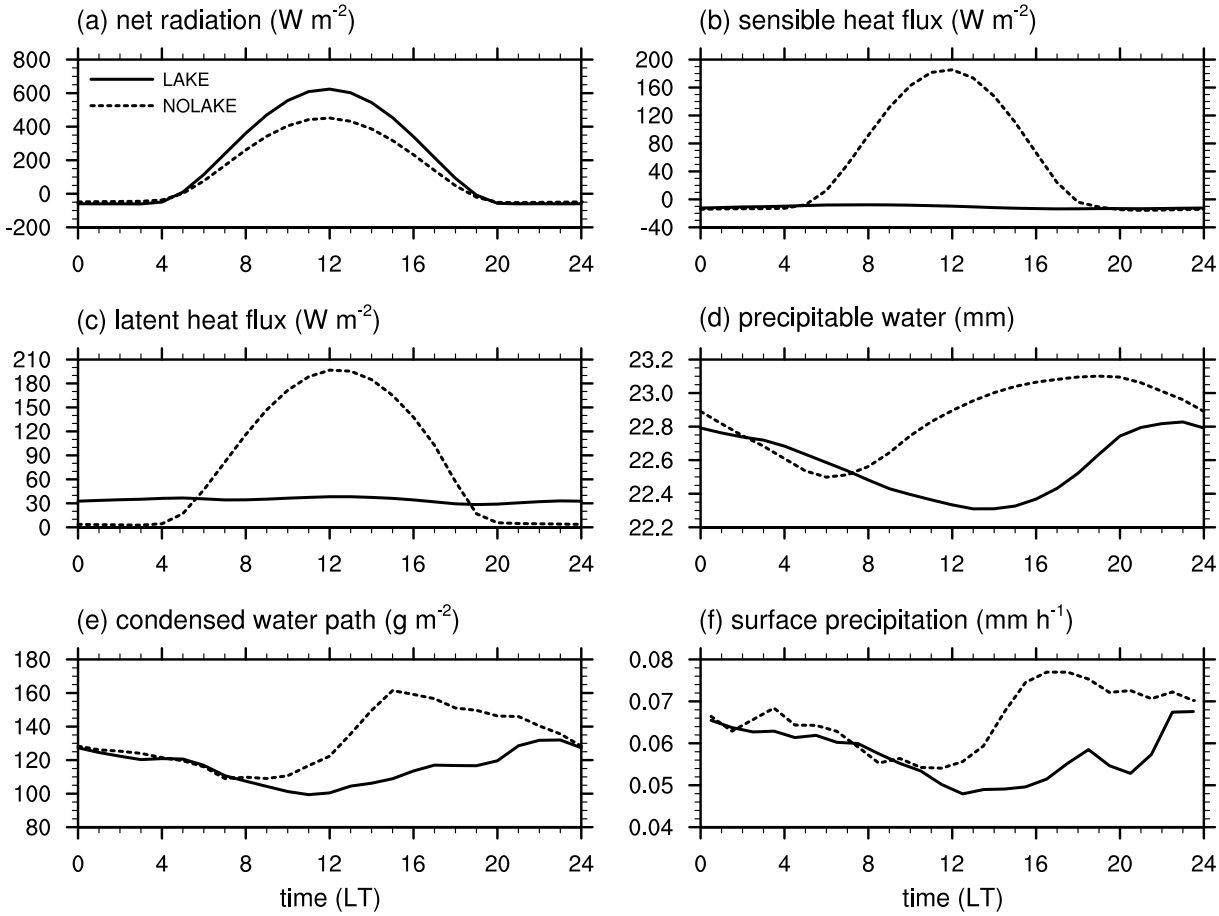

Figure 4. Diurnal variations of (a) net radiation at the surface, (b) surface sensible heat flux, (c) surface latent heat flux, (d) precipitable water (vertically integrated water vapor amount), (e) total (liquid plus ice) cloud water path, and (f) surface precipitation rate averaged over the Lake Baikal area in the LAKE (solid line) and NOLAKE (dashed line) simulations.

(Figure S7 in Supporting Information S1). The presence of the lake causes a general reduction in the mixing ratios of hydrometeors except for cloud water in the lower atmosphere (see also Figure 3b). The reduction of both the snow mixing ratio and the graupel mixing ratio by the lake can lead to the reduction of surface precipitation in the LAKE simulation via reduced melting.

4. Summary and Conclusions

The precipitation climatology estimated using satellite observations reveals that summertime surface precipitation over Lake Baikal is smaller than that over nearby areas. To understand the role of the lake in this precipitation reduction, here we employed the cloud-resolving numerical model and conducted two 15-year numerical simulations, one with the environment as is and the other with the environment in which the lake is replaced by forest. Except for some overestimations of the lake surface water temperature, the model represented the precipitation climatology and other observations generally well.

The simulations revealed that the lake decreases precipitation over its surface by 15%. Owing to its large heat capacity, the lake cools the atmosphere, and the cooling extends up to 2 km above its surface. This cooling leads to a more stable atmosphere, which is indicated by the decrease in PBL height and increased EPT slope in the lower layers. Because of the weakened convection along with the more stable atmosphere, moisture flux from the surface, which is associated with convection intensity, is smaller over the lake surface than over the forest-replaced surface. Owing to this decrease in moisture flux from the surface and decreased low-level moisture convergence due to the weakened convection, water vapor mixing ratio is decreased by the lake in the lower atmosphere up to 3 km above the surface. The lake enhances the net radiative flux at the surface, which is mostly

distributed by the heat flux descending into the deep lake water rather than sensible and latent heat fluxes to the atmosphere.

In this study, the lake model somewhat overestimated the lake surface water temperature, which may have been caused by model errors. Notwithstanding this issue, the model competently captured the atmospheric characteristics and demonstrated the horizontal and vertical extents and mechanisms of Lake Baikal's effects on precipitation climatology around it through representing complex interactions among physical processes. While more efforts should be put into developing and improving targeted models for replicating lake effects, this study demonstrated the value of using regional climate models to gain further insights into the impacts of surface properties on weather and climate.

Data Availability Statement

The satellite-based precipitation estimation data sets used in this study are available on the following links: PERSIANN-CDR (https://www.ncei.noaa.gov/products/climate-data-records/precipitation-persiann), IMERG-Final (https://disc.gsfc.nasa.gov/datasets/GPM_3IMERGDF_06/summary), CMORPH-CDR (https://www.ncei.noaa.gov/data/cmorph-high-resolution-global-precipitation-estimates/access/), GSMaP (https://sharaku.eorc.jaxa.jp/GSMaP/), and MSWEP (https://www.gloh2o.org/mswep/). The ERA5 data set is available on the link (https://cds.climate.copernicus.eu/cdsapp#!/dataset/reanalysis-era5-single-levels-monthly-means?tab=form). The model output is available via https://doi.org/10.17632/5cwk5myc6v.1.

Acknowledgments
The authors are thankful to the three anonymous reviewers for their valuable comments on this work. This work was supported by the National Research Foundation of Korea (NRF-2021R1A2C1007044 and NRF-2021R1C1C1012804). H.L was supported by the research grant of Kongju National University in 2020. G.G was partly supported by the Science and Technology Foundation of Mongolia (RUS/2019/14).

References

Ashouri, H., Hsu, K.-L., Sorooshian, S., Braithwaite, D. K., Knapp, K. R., Cecil, L. D., et al. (2015). PERSIANN-CDR: Daily precipitation climate data record from multisatellite observations for hydrological and climate studies. *Bulletin of the American Meteorological Society*, *96*(1), 69–83. https://doi.org/10.1175/BAMS-D-13-00068.1

Beck, H. E., Wood, E. F., Pan, M., Fisher, C. K., Miralles, D. G., van Dijk, A. I. J. M., et al. (2019). MSWEP V2 global 3-hourly 0.1° precipitation: Methodology and quantitative assessment. *Bulletin of the American Meteorological Society*, *100*(3), 473–500. https://doi.org/10.1175/BAMS-D-17-0138.1

Camberlin, P., Gitau, W., Planchon, O., Dubreuil, V., Funatsu, B. M., & Philippon, N. (2018). Major role of water bodies on diurnal precipitation regimes in Eastern Africa. *International Journal of Climatology*, *38*(2), 613–629. https://doi.org/10.1002/joc.5197

Dabaeva, D. B., Tsydypov, B. Z., Ayurzhanaev, A. A., Andreev, S. G., & Garmaev, Y. Z. (2016). Peculiarities of Lake Baikal water level regime. *IOP Conference Series: Earth and Environmental Science*, *48*, 012014. https://doi.org/10.1088/1755-1315/48/1/012014

Gu, H., Jin, J., Wu, Y., Ek, M. B., & Subin, Z. M. (2015). Calibration and validation of lake surface temperature simulations with the coupled WRF-lake model. *Climatic Change*, *129*(3–4), 471–483. https://doi.org/10.1007/s10584-013-0978-y

Gu, H., Ma, Z., & Li, M. (2016). Effect of a large and very shallow lake on local summer precipitation over the Lake Taihu basin in China. *Journal of Geophysical Research: Atmospheres*, *121*(15), 8832–8848. https://doi.org/10.1002/2015JD024098

Hansen, M. C., DeFries, R. S., Townshend, J. R. G., & Sohlberg, R. (2000). Global land cover classification at 1 km spatial resolution using a classification tree approach. *International Journal of Remote Sensing*, *21*(6–7), 1331–1364. https://doi.org/10.1080/014311600210209

Hawcroft, M. K., Shaffrey, L. C., Hodges, K. I., & Dacre, H. F. (2012). How much Northern Hemisphere precipitation is associated with extratropical cyclones? *Geophysical Research Letters*, *39*(24), L24809. https://doi.org/10.1029/2012GL053866

Hersbach, H., Bell, B., Berrisford, P., Hirahara, S., Horányi, A., Muñoz-Sabater, J., et al. (2020). The ERA5 global reanalysis. *Quarterly Journal of the Royal Meteorological Society*, *146*(730), 1999–2049. https://doi.org/10.1002/qj.3803

Huffman, G. J., Bolvin, D. T., Nelkin, E. J., & Tan, J. (2020). *Integrated Multi-satellitE Retrievals for GPM (IMERG) technical documentation*. NASA Goddard Space Flight Center. Retrieved from https://gpm.nasa.gov/sites/default/files/2020-10/IMERG_doc_201006.pdf

Kalnay, E., Kanamitsu, M., Kistler, R., Collins, W., Deaven, D., Gandin, L., et al. (1996). The NCEP/NCAR 40-year reanalysis project. *Bulletin of the American Meteorological Society*, *77*(3), 437–472. https://doi.org/10.1175/1520-0477(1996)077<0437:TNYRP>2.0.CO;2

Kouraev, A. V., Semovski, S. V., Shimaraev, M. N., Mognard, N. M., Legrésy, B., & Rémy, F. (2007). The ice regime of Lake Baikal from historical and satellite data: Relationship to air temperature, dynamical, and other factors. *Limnology & Oceanography*, *52*(3), 1268–1286. https://doi.org/10.4319/lo.2007.52.3.1268

Kouraev, A. V., Zakharova, E. A., Kostianoy, A. G., Shimaraev, M. N., Desinov, L. V., Petrov, E. A., et al. (2021). Giant ice rings in southern Baikal: Multi-satellite data help to study ice cover dynamics and eddies under ice. *The Cryosphere*, *15*(9), 4501–4516. https://doi.org/10.5194/tc-15-4501-2021

Kubota, T., Aonashi, K., Ushio, T., Shige, S., Takayabu, Y. N., Kachi, M., et al. (2020). Global satellite mapping of precipitation (GSMaP) products in the GPM era. In V. Levizzani, C. Kidd, D. B. Kirschbaum, C. D. Kummerow, K. Nakamura, & F. J. Turk (Eds.), *Satellite precipitation measurement, advances in global change research* (Vol. 67, pp. 355–373). Springer. https://doi.org/10.1007/978-3-030-24568-9_20

Laird, N. F., Desrochers, J., & Payer, M. (2009). Climatology of lake-effect precipitation events over Lake Champlain. *Journal of Applied Meteorology and Climatology*, *48*(2), 232–250. https://doi.org/10.1175/2008JAMC1923.1

Lyons, W. A. (1966). *Some effects of Lake Michigan upon squall lines and summertime convection, satellite and mesometeorology research project*. University of Chicago.

Nicholson, S. E., Klotter, D., & Hartman, A. T. (2021). Lake-effect rains over Lake Victoria and their association with mesoscale convective systems. *Journal of Hydrometeorology*, *22*(6), 1353–1368. https://doi.org/10.1175/JHM-D-20-0244.1

Notaro, M., Holman, K., Zarrin, A., Fluck, E., Vavrus, S., & Bennington, V. (2013). Influence of the Laurentian Great Lakes on regional climate. *Journal of Climate*, *26*(3), 789–804. https://doi.org/10.1175/JCLI-D-12-00140.1

Peace, R. L., Jr., & Sykes, R. B., Jr. (1966). Mesoscale study of a lake effect snow storm. *Monthly Weather Review*, *94*(8), 495–507. https://doi.org/10.1175/1520-0493(1966)094<0495:MSOALE>2.3.CO;2

Samuelsson, P., Kourzeneva, E., & Mironov, D. (2010). The impact of lakes on the European climate as simulated by a regional climate model. *Boreal Environment Research*, *15*, 113–129.

Satyamurty, P., da Costa, C. P. W., & Manzi, A. O. (2013). Moisture source for the Amazon Basin: A study of contrasting years. *Theorerical and Applied Climatology*, *111*(1–2), 195–209. https://doi.org/10.1007/s00704-012-0637-7

Skamarock, W. C., Klemp, J. B., Dudhia, J., Gill, D. O., Liu, Z., Berner, J., et al. (2019). *A description of the advanced research WRF version 4 (No. NCAR/TN-556+STR)*. National Center for Atmospheric Research. https://doi.org/10.5065/1dfh-6p97

Steenburgh, W. J., Halvorson, S. F., & Onton, D. J. (2000). Climatology of lake-effect snowstorms of the Great Salt Lake. *Monthly Weather Review*, *128*(3), 709–727. https://doi.org/10.1175/1520-0493(2000)128<0709:COLESO>2.0.CO;2

Tewari, M., Chen, F., Wang, W., Dudhia, J., LeMone, M. A., Mitchell, K., et al. (2004). *Implementation and verification of the unified NOAH land surface model in the WRF model*. Paper presented at 20th Conference on weather analysis and forecasting/16th conference on numerical weather prediction. American Meteorological Society.

Thiery, W., Davin, E. L., Panitz, H.-J., Demuzere, M., Lhermitte, S., & van Lipzig, N. (2015). The impact of the African Great Lakes on the regional climate. *Journal of Climate*, *28*(10), 4061–4085. https://doi.org/10.1175/JCLI-D-14-00565.1

Van de Walle, J., Thiery, W., Brousse, O., Souverijns, N., Demuzere, M., & van Lipzig, N. P. M. (2020). A convection-permitting model for the Lake Victoria Basin: Evaluation and insight into the mesoscale versus synoptic atmospheric dynamics. *Climate Dynamics*, *54*(3–4), 1779–1799. https://doi.org/10.1007/s00382-019-05088-2

Xie, P., Joyce, R., Wu, S., Yoo, S.-H., Yarosh, Y., Sun, F., & Lin, R. (2017). Reprocessed, bias-corrected CMORPH global high-resolution precipitation estimates from 1998. *Journal of Hydrometeorology*, *18*(6), 1617–1641. https://doi.org/10.1175/JHM-D-16-0168.1

References From the Supporting Information

Carrea, L., & Merchant, C. J. (2019). Globolakes: Lake Surface Water Temperature (LSWT) v4.0. [Dataset]. Centre for Environmental Data Analysis, 1995–2016. https://doi.org/10.5285/76a29c5b55204b66a40308fc2ba9cdb3

Hong, S.-Y., & Lim, J.-O. J. (2006). The WRF single-moment 6-class microphysics scheme (WSM6). *Journal of the Korean Meteorological Society*, *42*, 129–151.

Hong, S.-Y., Noh, Y., & Dudhia, J. (2006). A new vertical diffusion package with an explicit treatment of entrainment processes. *Monthly Weather Review*, *134*(9), 2318–2341. https://doi.org/10.1175/MWR3199.1

Iacono, M. J., Delamere, J. S., Mlawer, E. J., Shephard, M. W., Clough, S. A., & Collins, W. D. (2008). Radiative forcing by long-lived greenhouse gases: Calculations with the AER radiative transfer models. *Journal of Geophysical Research*, *113*(D13). https://doi.org/10.1029/2008jd009944

Jiménez, P. A., Dudhia, J., González-Rouco, J. F., Navarro, J., Montávez, J. P., & García-Bustamante, E. (2012). A revised scheme for the WRF surface layer formulation. *Monthly Weather Review*, *140*(3), 898–918. https://doi.org/10.1175/MWR-D-11-00056.1

Kain, J. S. (2004). The Kain–Fritsch convective parameterization: An update. *Journal of Applied Meteorology and Climatology*, *43*(1), 170–181. https://doi.org/10.1175/1520-0450(2004)043<0170:TKCPAU>.0.CO;2